# Signature of stripes in the optical conductivity of $La_2NiO_{4.11}$

Nathalie Poirot-Reveau,[1,2,*] Philippe Odier,[3] Patrick Simon,[4] and François Gervais[1]
[1]*Laboratory of Electrodynamics of Advanced Materials, FRE2077 CNRS, CEA LRC M01, Faculty of Sciences & Techniques, François-Rabelais University, Parc de Grandmont, 37200 Tours, France*
[2]*University Institute of Technology, François Rabelais University, 41000 Blois, France*
[3]*Laboratoire de Cristallographie, CNRS, 25 av des martyrs, BP 166, F-38042 Grenoble cedex 09, France*
[4]*Centre de Recherches sur les Matériaux à Haute Temperature, CNRS, 45071 Orléans cédex 2, France*
(Received 25 July 2000; revised manuscript received 4 May 2001; published 1 February 2002)

The temperature dependence of the infrared reflectivity spectra of a single crystal of $La_2NiO_{4+\delta}$, with an oxygen excess $\delta=0.11$, is analyzed by both Kramers-Kronig analysis and an attempt to fit with optical conductivity models for the polarization within the basal plane. This oxygen excess corresponds to a composition of the phase diagram where stripe formation has been reported by other methods. In particular, highly anomalous low-frequency tails of incompletely screened phonon responses are suspected to be the signature of static charge stripes, treated here as multipolarons. By comparison with the positions of extra peaks and with the dispersion curve of phonons, a charge-order wave vector $Q$ has been determined. More generally, the analysis allows us to discriminate trapped and mobile charge carriers. A change of regime from mobile to trapped polarons upon cooling is evidenced. Two thresholds in the temperature dependence of relevant parameters and/or data are evidenced for this sample. One is assigned to charge ordering and the other confirms the onset of combined charge and spin order reported at low temperature by other methods.

DOI: 10.1103/PhysRevB.65.094503 PACS number(s): 74.25.Gz, 71.38.−k

## INTRODUCTION

Many recent observations in doped copper,[1] nickel,[2] or manganese[3] oxide compounds derived from the prototypic perovskite structure suggest that the minimization of the energy of the system is accommodated by a combined order of holes and spins. The system reaches an energy state downshifted by hole segregation[4–8] and, therefore, becomes heterogeneous. As a result, a stripe ordering has been proposed:[9,10] it consists of a segregation of charges in domains walls which separate periodically nondoped antiferromagnetic (AF) domains with a period related to the carrier density. This stripe order has been shown to be a current phenomenon in the cuprates[1,11–13] and nickelates.[2,6,14–18] As a result the system is incommensurate or commensurate depending on the wave vector characterizing the stripe structure. Since this ''phase separation'' allows the coexistence of superconductivity and of long-range ordered AF domains, it may play a key role in the mechanism of HTSC itself by discarding the puzzling problem of pair breaking. More generally, these stripe phases raise several questions about their formation. The first experimental observation of unusual magnetic correlation in the nickelates was realized by Hayden *et al.*[17] by neutron diffraction on the $La_{2-x}Sr_xNiO_{3.96}$ crystal. The existence of a hole order in $La_{2-x}Sr_xNiO_4$ was confirmed by electron-diffraction[2] and transport measurements.[19] Here we report spectroscopic observations in overstoichiometric $La_2NiO_{4+\delta}$, with $\delta=0.11$, that belong to a stripe phase which has been the object of few reports.[20,21] The analysis of infrared reflectivity for the polarization within the basal plane shows the unambiguous signature of the folding of the incommensurate wave vector at the Brillouin-zone center. These observations confirm and complete a recent study where one phonon made active by Brillouin-zone folding was shown to interfere in the Fano sense with the electronic continuum of the charges within a stripe.

As for prototypic cuprate discovered by Berdnorz and Müller,[22] the symmetry of the $La_2NiO_4$ structure is tetragonal $I4/mmm$. It consists of a successive stacking of $BO_2$ layers and $A_2O_2$ block layers of the NaCl type. This compound, which is a two-dimensional antiferromagnet, may be hole doped by two methods: divalent cation-doping onto the La site or insertion of additional oxygen atoms ($O_i$) between LaO layers.[23,24] Doping contributes to the relaxation of structural strains,[25,26] and confers electronic and magnetic properties to the materials. Their understanding, to the best of our knowledge, does not yet give rise to a consensus, in spite of an enormous effort during the last decade. In the $La_2MO_{4+\delta}$ ($M=$Cu, Ni) system, stable phases with high $\delta$ exist because the arrangement of interstitial oxygen at short or long distance allows different possibilities of tilting for $MO_6$ octahedra. Different crystal structures with well-defined phases were observed depending on the doping level. Structures showing oxygen excess ordering in $La_2NiO_{4+\delta}$ were identified by several groups.[4,5] Odier *et al.* proposed the $T$-$\delta$ phase diagram summarized in Fig. 1 (Ref. 20). Due to hole injection in the AF matrix, $La_2NiO_{4+\delta}$ shows incommensurate phases depending on their concentration, and commensurate systems for specific concentrations. In $La_2NiO_{4+\delta}$ with $\delta=0.131$, 0.135, and 0.141, the charge ordering proceeds gradually upon cooling without any phase transition,[27] contrary to $La_{0.5}Sr_{1.5}MnO_4$ (Refs. 28 and 29) compound, for example. The stripe order in $La_2NiO_{4+\delta}$ is incommensurate, with a wave vector depending on temperature.[6,18] The magnetic modulation parameter also depends on the hole concentration ($n_h=x+2\delta$).[30] The total length of the domain walls is proportional to the hole rate $\delta\sim 1/d$, d being the distance separating the domain walls. The correlation length in the plane increases with the $n_h$

 

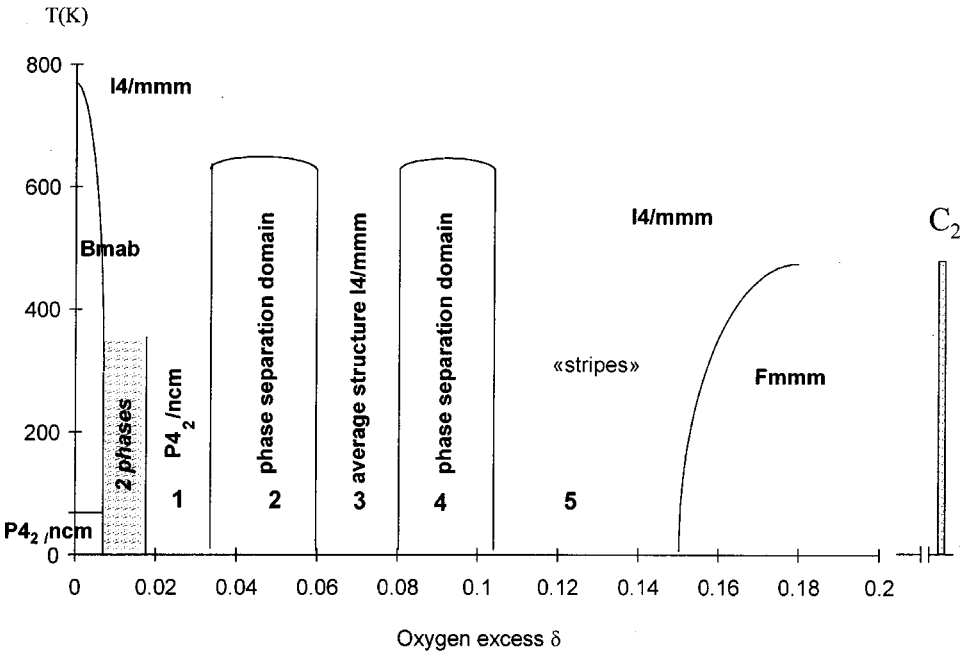


FIG. 1. Proposed structural phase diagram for $La_2NiO_{4+\delta}$ (Ref. 20).

doping in the Sr-doped crystal. The extrapolation indicates a maximal correlation length for $n_h=0.25$, what corresponds to $\delta=0.133$ for oxygen doping, close to the limit of crossover of the commensurate phase to the incommensurate stripe order. The domain walls may be centered on the Ni-atom lines (stripes centered on the sites) or on the lines of oxygen atoms (stripes centered on the bonds). For a domain wall centered on the oxygen bonds, a configuration where a resulting magnetic moment is nonzero is highly suggested.[31,32] Recently, it was shown that nickelates[33] may be in a mixed state of both stripe phases, the Ni-centered stripe phase being favored when the temperature decreases and with a higher electron-phonon coupling constant. For the $La_2NiO_{4.133}$ compound, a charge order at $T\leqslant 220$ K with a magnetic modulation parameter equal to $\frac{1}{3}$, and a magnetic order at $T_m=110.5$ K has been evidenced by neutron diffraction.[34] The modulation vector direction indicates that the stripes are along the [110] direction in the $NiO_2$ plane, contrary to the [100] direction in cuprates. Incommensurability in $La_2NiO_{4+\delta}$ assumes a wave vector $Q$ varying with both doping and temperature.[6,18] Many neutron studies showed clear evidence of the existence of stripes by the presence of additional diffraction peaks below the charge-ordering temperature $T_{co}$. These stripes lower the crystal symmetry and activate extra lines in the infrared spectra. Recently Katsufuji *et al.*[14] observed, in $La_{2-x}Sr_xNiO_4$ compounds, the signature of a charge order at 240 K in the optical conductivity via the splitting of an optic phonon $E_u$ located at 354 $cm^{-1}$ (the bending mode of the Ni-O octahedron), assigned to a reduction of the crystal symmetry. These results were confirmed in Ref. 35 by phonon Raman scattering. The observed dependence on temperature confirms that the spin ordering is driven by charge ordering and that fluctuating stripes persist above the ordering transition. In the same compound, Yamamoto *et al.*[36] showed, by Raman scattering, the appearance of phonons in $A_{1g}$ symmetry below $T_{co}$ attributed to the lattice distortion associated with charge ordering. More recent infrared and Raman investigations[37] showed the extra phonon peaks induced by stripe order in conductivity spectra. One peak even presents a strong Fano antiresonance attributed to electron-phonon coupling. These results indicate that stripe ordering strongly affects the electronic response of the compound, and is associated with conducting character of stripes.

Unlike isostructural $La_2CuO_4$, lanthanum nickelate remains insulating at low temperature up to high doping levels. As a result, and again contrary to cuprates, no Drude or Drude-like profile screens the phonons at low temperature in infrared reflection spectra. It was often suggested[38] that the principal difference between cuprates and nickelates is the larger electron-phonon coupling in nickelates. Even if these compounds are electrical conductors at room temperature and above, their low ratio carrier concentration over effective mass does not rank them as conventional metals. The same conclusion comes from the temperature dependence of the resistivity, which increases upon cooling, at-least if, for the definition of the metal, one adopts an electronic concentration that shifts the plasma edge up to the ultraviolet region, thus allowing the metal to display a typical ''metallic-type'' reflectivity in the visible spectrum. Conversely, all of these conducting oxides are black, meaning that charge carriers absorb radiation but are not numerous enough to oscillate as a plasmon mode to reflect radiation. Here the equivalent of the plasma edge stays in the near infrared. Another key point that causes a decisive difference from conventional metal is the incomplete screening. In metals, the charge carriers do not interact with each other. Electrostatic interactions are completely screened. The screening is usually expressed by a term that exponentially lowers the electrostatic interaction potential vs distance, parametrized via the Thomas-Fermi wave vector. As a result, phonons are also screened in conventional metals. The situation appears entirely different in conducting oxides. Charge carriers do interact and polar phonons are incompletely screened. As a result, the polaron

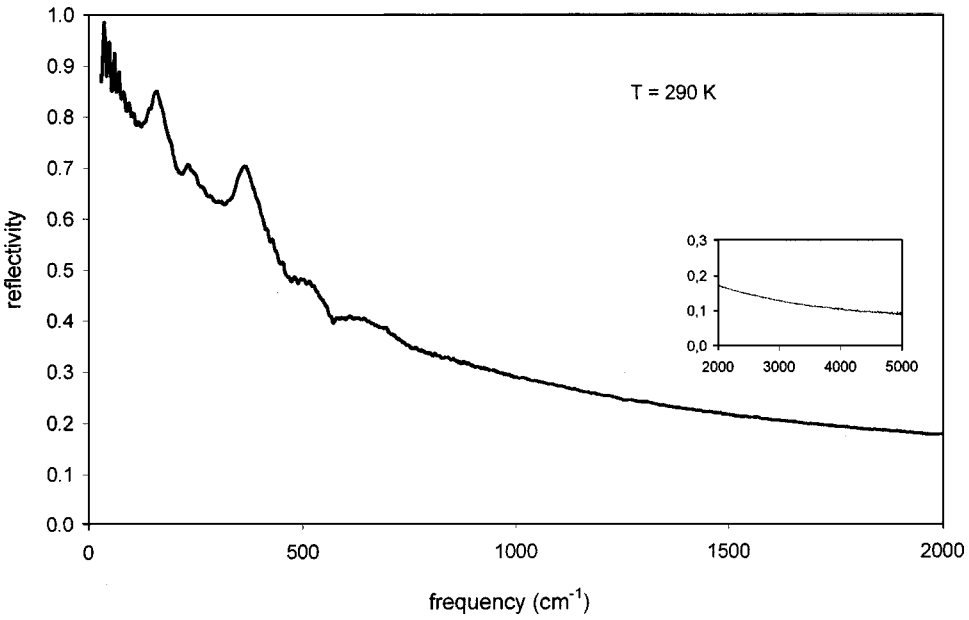


FIG. 2. Infrared reflectivity spectrum at 300 K obtained for on a $(a,b)$ plane with $\delta = 0.11$.

concept is expected to replace the conventional metal concept. The observed band in midinfrared in oxide conductors and HTSC, may be attributed, therefore, to a polaron signature.[39–44] In this framework, a stripe may be viewed as a chain of polarons.

The temperature dependence of infrared reflectivity in a $La_2NiO_{4.11}$ single crystal will be reported here. We will attempt to fit the reflectivity with a model allowing us to discriminate between itinerant and trapped polarons. Data will be analyzed in terms of optical conductivity and by comparison with results available with the same method on parent samples with different oxygen dopings. Anomalies will be searched close to 150 K, where a charge order phenomenon is expected as reported elsewhere in the same sample by other methods.[21] Phonon anomalies are also expected, as the signature of this dynamic-static transition.

## RESULTS AND DISCUSSION

Single crystals were prepared by the melting zone technique.[45] They were cut into slices oriented by the Laüe method. The $(a,b)$ plane was then polished optically with SiC disks and a suspension of 1-$\mu$m diamond powder for final polishing. In order to obtain the expected oxygen excess in these materials, an annealing at 300–400 °C for several hours under a 80%Ar+20%$H_2$ atmosphere is used with a reference crystal sample. Their oxygen excess $\delta$ was deduced from a TGA analysis of the reference crystal sample by measuring the weight variation in a total reduction under a 95%Ar+5%$H_2$ atmosphere. We have studied a $La_2NiO_{4+\delta}$ single crystal with $\delta = 0.11$ by infrared reflectivity between 4 and 290 K, from 20 to 7000 $cm^{-1}$, with the electric field of the electromagnetic radiation parallel to the $(a,b)$ plane. The

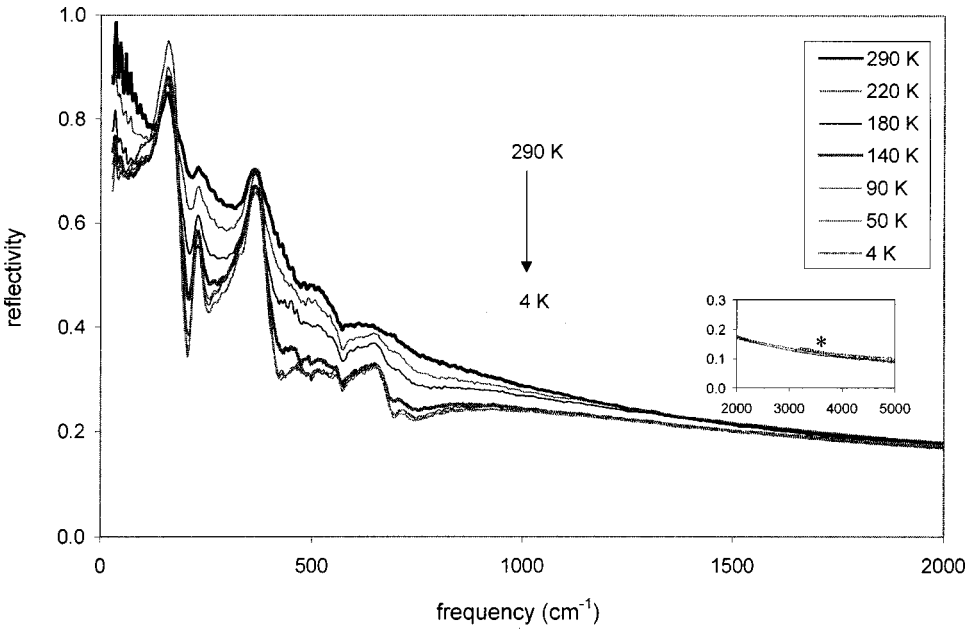


FIG. 3. Reflectivity spectra for temperatures ranging between 290 and 4 K, obtained for an electric field of the infrared radiation within an $a$-$b$ plane for the sample with $\delta = 0.11$. Inset: data between 2000 and 5000 $cm^{-1}$.*Jumps due to the connection between experimental data.

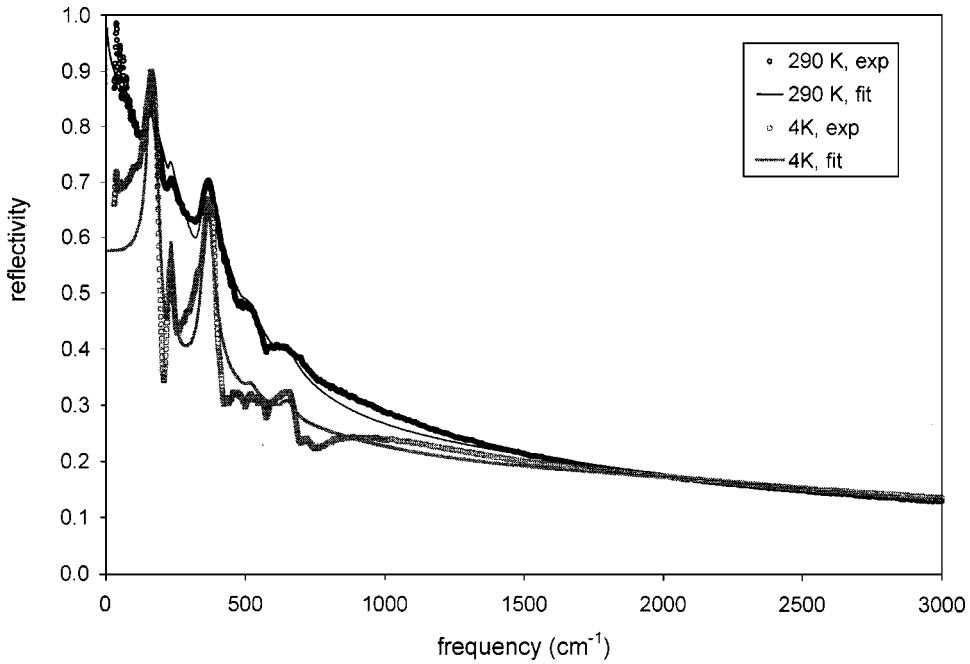


FIG. 4. Experimental data and best data fit at 290 and 4 K; $(a,b)$ plane; $\delta=0.11$.

reflectivity spectra have been obtained with a Fourier transform infrared spectrometer BRUKER IFS 113. Spectra have been fitted with the dielectric function model

$$\tilde{\varepsilon}(\omega)=\varepsilon_\infty\left[\prod_j \frac{\Omega_{j\mathrm{LO}}^2-\omega^2+i\gamma_{j\mathrm{LO}}\omega}{\Omega_{j\mathrm{TO}}^2-\omega^2+i\gamma_{j\mathrm{TO}}\omega}-\frac{\Omega_P^2+i(\gamma_P-\gamma_0)\omega}{\omega(\omega-i\gamma_0)}\right]. \quad (1)$$

Attempts to fit with more conventional models summing over Lorentzian oscillators and conventional Drude models indeed failed. As we will see later, several peaks show asymmetric profiles which may be described correctly, at least to some extent, with the model above. Typical experimental data at room temperature are shown in Fig. 2. At high frequency, the level of reflectivity is comparable with that of published works on nickelate[44,46] and cuprate[39,40,47] compounds, with a high frequency dielectric constant $\varepsilon_\infty$ varying from 3.2 to 3.5 in the present compound depending on temperature. Actually, if present $\varepsilon_\infty$'s are similar to the value found in current cuprates [$\varepsilon_\infty=3.6$ for the $(a,b)$ plane of $YBa_2Cu_3O_7$, for example],[48] it is found to be lower than that of nickelate compounds already published (4.5–5) by two of the authors.[46] Neither of the previous studies focused on the specific composition studied here, however. To our knowledge, this is the first indication of the uncommon behavior of the studied composition, as will be discussed below. Low reflectivity levels in the range 0.5–1.2 eV were also observed in overstoichiometric $La_2CuO_{4+\delta}$.[49] Here the difference between the value $\varepsilon_\infty=3.2$–$3.5$ and the value 4.5–5 of nickelates of different stoichiometry is sufficiently large to ex-

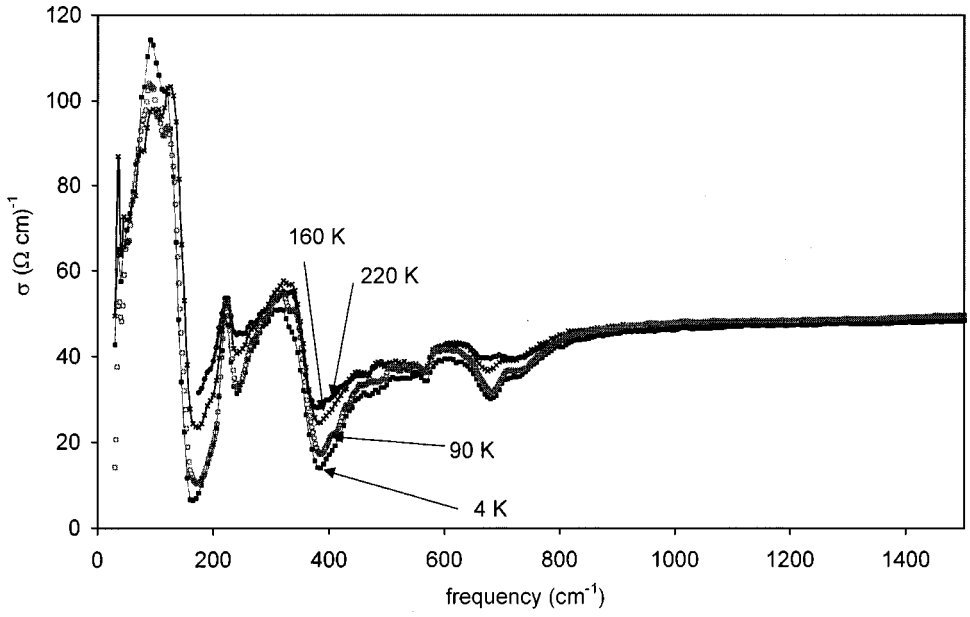


FIG. 5. Optical conductivity obtained by a Kramers-Kronig analysis of the reflectivity data.

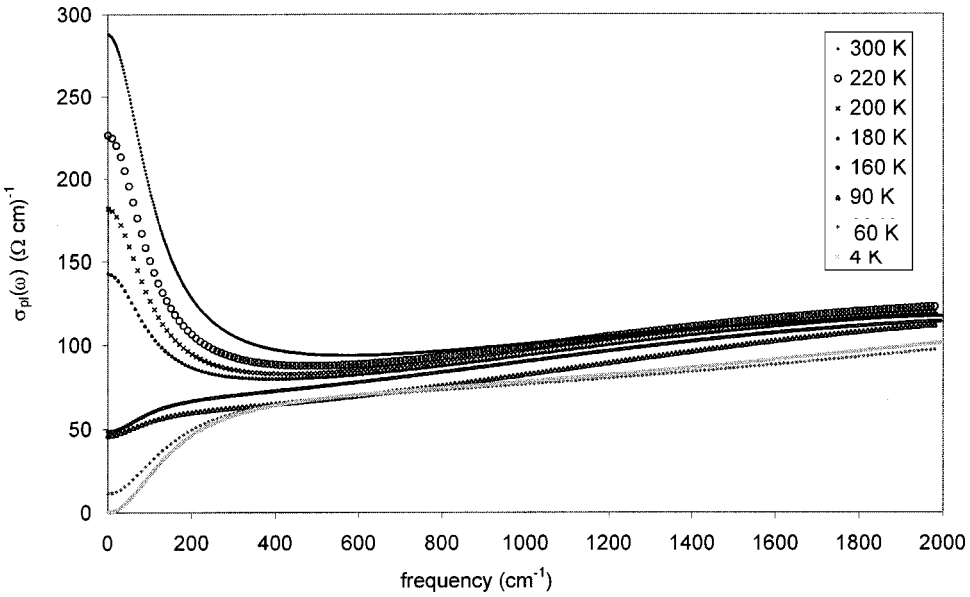


FIG. 6. Plasmon contribution to the real part of the spectral conductivity with the temperature.

clude the usual error sources of absolute reflectivity measurements: (i) a geometric misalignment would lead to a zero-frequency limit of the reflectivity strongly different from 1 in the conducting regime (see Fig. 4 at 290 K), and (ii) losses due to diffuse reflectance on a rough surface cannot induce such a difference in the spectral range 20–3000 $cm^{-1}$ covered in the fitting process: the surface would appear rough to the eye. This was not the case, and the procedure of polishing and measurements was similar to previous reports in the same group, particularly on insulating materials where the flat reflectivity level expected in the transparency range above phonons is a good probe of the quality of the polishing procedure. The low reflectivity at high energy appears, therefore, intrinsic to this compound. Nevertheless, note that the main conclusions of the paper, i.e., especially all temperature dependences, would not be changed (expect $\varepsilon_\infty$, of course) if one would decide to artificially increase the high-frequency reflectivity up to a factor of 2. The dependence of the spectral reflectivity on temperature is shown in Fig. 3. The optical conductivity $\sigma(\omega)$ is then deduced from the dielectric response $\varepsilon(\omega)$ via

$$\tilde{\varepsilon}(\omega)=1-\frac{i\tilde{\sigma}(\omega)}{\varepsilon_v\omega}, \tag{2}$$

with $\varepsilon_v$ the vacuum dielectric permittivity. The model of Eq. (1) allows us to discriminate local oscillators like phonons or trapped polarons via the first term, while the second, inherited from the Drude model, describes the mobile charge carriers. The ''double-damping'' second term allows a good fit of spectra of all oxide conductors investigated up to now,[43–44,48,50–52] whereas the conventional Drude model ($\gamma_P=\gamma_0$) systematically failed. However, the model is unable to fit the low-temperature data of the present series of measurements, as shown in Fig. 4. Actually the model fits the data well above 160 K but for spectra below this temperature

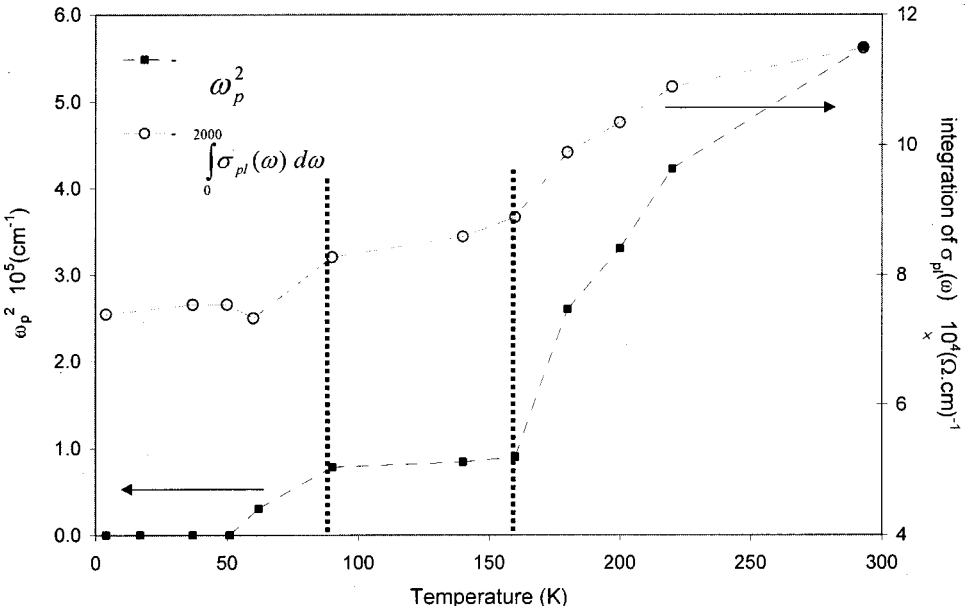


FIG. 7. Plasma frequency squared vs temperature. The dotted lines indicate the changes of the regime. Selected contributions to the integrated intensity.

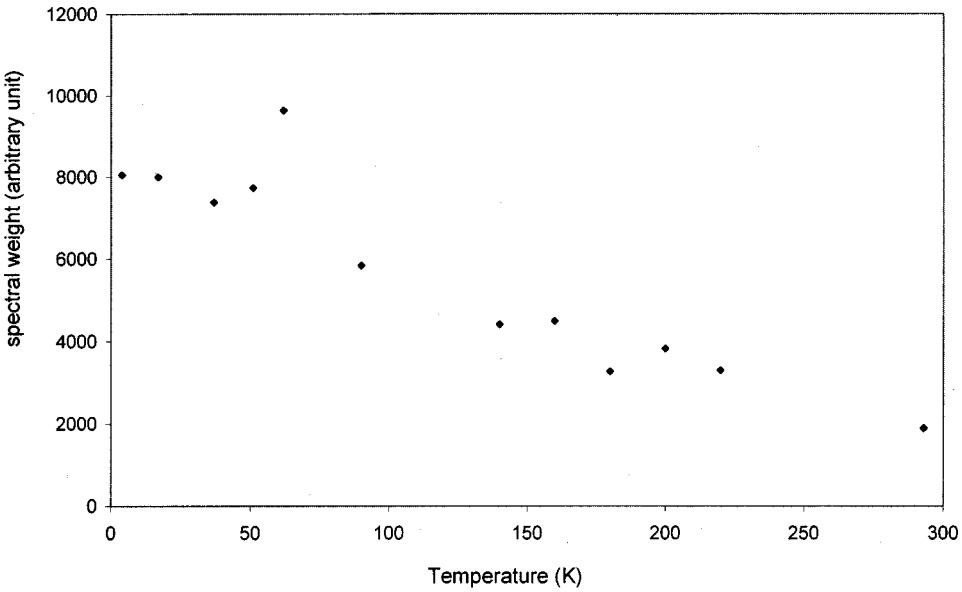


FIG. 8. Temperature dependence of the spectral weight of the phonons.

no acceptable fit can be achieved.[53] The origin of the disagreement appears straightforward. The peaks are very asymmetric, with a shoulder in the low-frequency tail. The optical conductivity $\sigma(\omega)$ obtained from Kramers-Kronig inversion is shown in Fig. 5. The model of Eq. (1) allows us to discriminate different contributions of the optical conductivity: a midinfrared band, phonons, and mobile charge carriers. The plasmon contribution [the second term on the right-hand side of Eq. (1)] of the real part of the spectral conductivity $\sigma_{\mathrm{pl}}(\omega)$ (see Fig. 6), which decreases with temperature, especially when the frequency approaches zero, indicates that the compound becomes insulator with the localization of charges at a temperature close to 160 K. Integration of the plasmon contribution to the real part of the spectral conductivity, and the square plasma frequency $\Omega_p^2$ vs temperature, are plotted in Fig. 7. This last quantity is expected—within a Drude description—to scale with the spectral weight of mobile charge carriers. Three regimes are shown. The first anomaly, close to 160 K, is attributed to a localization of charges and/or to itinerant polarons becoming trapped; the second anomaly is attributed to a combined charge and spin order. An anomaly at 60 K in the integrated plasmon conductivity is observed. The temperature dependence of the spectral weight in the phonon region is shown in Fig. 8. The increase of additional intensity with decreasing temperature is too large to be assigned to the normal temperature dependence of phonons. At 60 K, an anomaly shows up, and can be connected with what is observed in the integrated conductivity. Figure 9 indeed does not show any tendency at phonon mode softening. The present spectrum (Fig. 4) resembles others already reported by the Calvani group concerning cuprate single crystals at low temperature.[39,47,57] They were interpreted in terms of additional spectral weight assigned to charges bound to the lattice via a polaronic coupling. This phenomenon is unambiguously confirmed in our series of spectra. In addition, our fitting procedure allows us to dis-

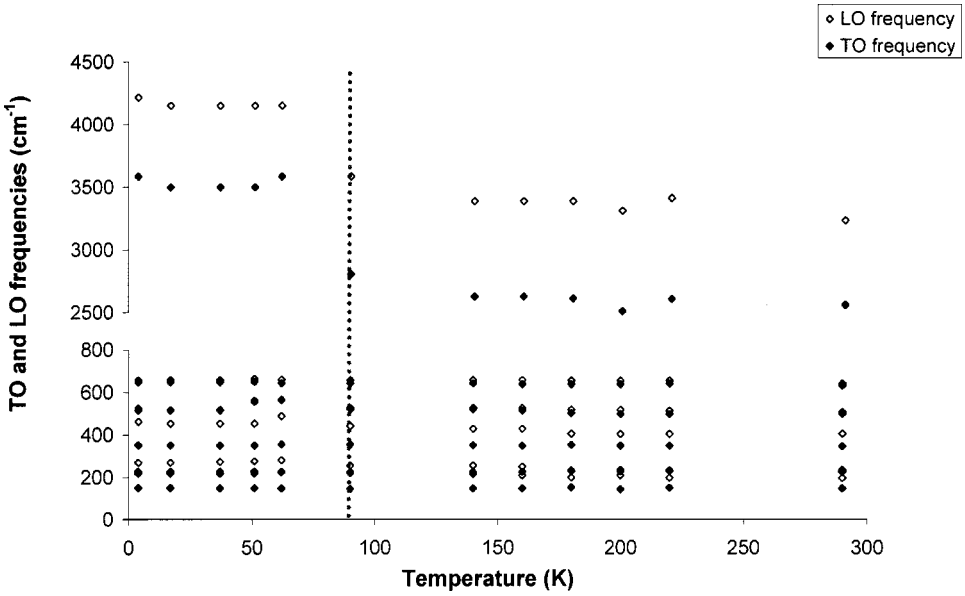


FIG. 9. Temperature dependence of LO- and TO-phonon frequencies.

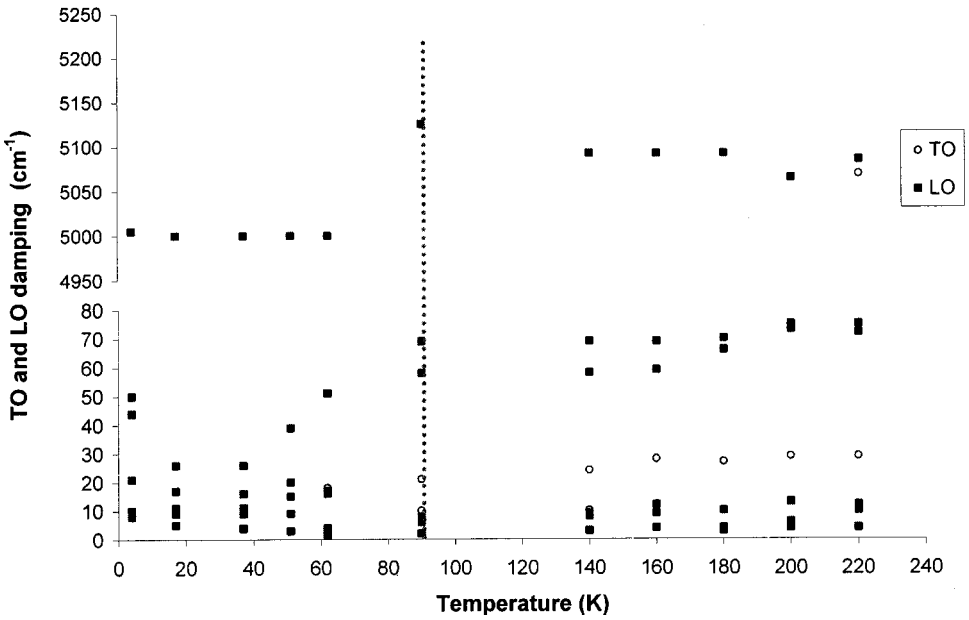


FIG. 10. Selected TO and LO dampings vs temperature. The dotted line indicates the cutoff of change of regime.

criminate several tendencies and regimes.

(i) A Drude-like component in the conductivity is observed in the temperature range from 300 K down to 180 K. Its contribution to the spectral weight decreases upon cooling. By ''Drude-like'' we mean a conductivity that increases upon decreasing frequency yielding a zero-frequency-centered broad peak. In the temperature range from 160 K down to 62 K, the static conductivity is nonzero but definitely non-Drude-like in that the conductivity decreases upon decreasing frequency. Below 50 K, the conductivity extrapolates to negligible value at zero frequency.

(ii) Additional contributions appearing as low-frequency shoulders of the phonon peaks are observed at room temperature. Their intensity grows upon cooling to become so large that Eq. (1) becomes unable to fit the data below 160 K.

(iii) A broad midinfrared band is confirmed.

In the literature, the relative decrease of spectral weight at low frequency with respect to an expected Drude-like response is often assigned to a charge pseudogap. This model was widely discussed for the *c*-axis polarization of underdoped cuprates (see a recent discussion in Ref. 54 and references therein, for example). The discussion about the pseudo-gap has been extended to the (*a*,*b*) plane.[55–57] The opening of a gap in the conductivity upon cooling appears compatible with our observations. However, should the non-Drude-like behavior be treated as a lack of response in the optical conductivity (or in the scattering rate) within a pseudogap picture description, as proposed by many authors? Or should we consider that the mobile charge-carrier response varies continuously from Drude-like at room temperature to incoherent scattering at low temperature (a roughly flat response) plus midinfrared bands and far-infrared additional response assigned to trapped polarons? Actually, the answer might be a delicate balance of several contributions, as suggested by ''atypical'' behaviors exemplified initially in a $La_2CuO_{4.06}$ single crystal,[49] and confirmed

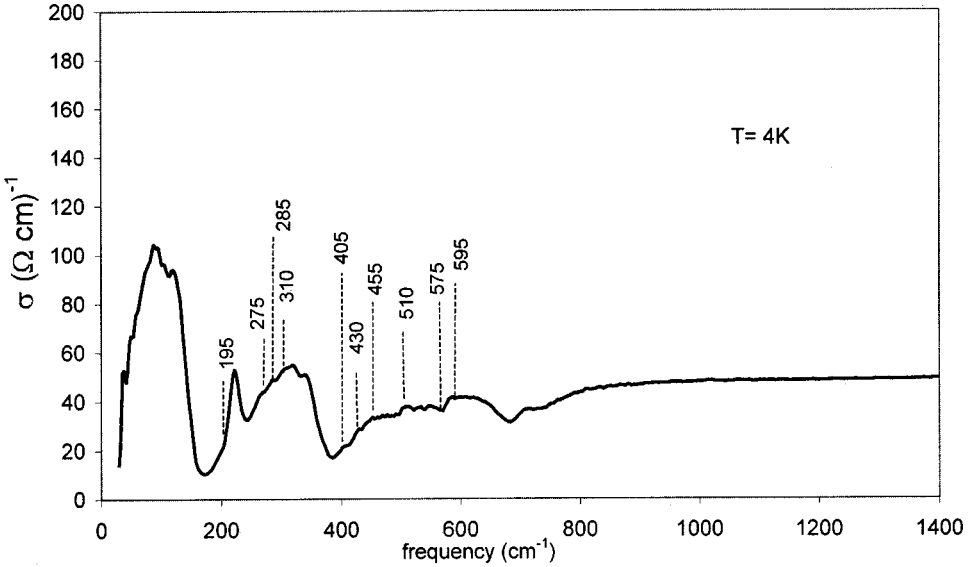


FIG. 11. Optical conductivity obtained by a Kramers-Kronig analysis of the reflectivity data at 4 K. The dashed lines indicate the positions in frequency of shoulders.

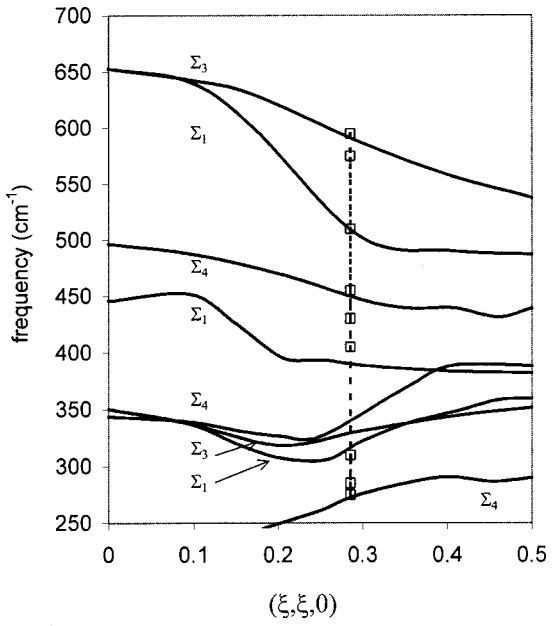


FIG. 12. Comparison of extra peaks positions observed in conductivity spectra (squares) with highest phonon branches along ($\xi$, $\xi$, 0) measured for $La_2NiO_4$ from Ref. 59.

lately,[56,57] in all cases for the ($a$,$b$) plane as in the present study. In those examples, the optical conductivity becomes more Drude-like at low temperature with the onset of a central peak, than at room temperature where a ''pseudogap'' develops in the conductivity. The very asymmetric phonon (or pseudophonon) lines observed here at low temperature are very uncommon. They were definitely observed in the Calvani group reports, but not in many other investigations of other compounds of the nickelate and cuprate families, neither by us nor by others. In particular, the authors of Ref. 44 were able to fit the temperature dependence of $Pr_2NiO_{4.22}$ with the model of Eq. (1) without any problem, meaning that anomalies in the phonon region are not observed for this composition. They interpreted the midinfrared band as a polaron signature. Preliminary studies showed that the phase diagram of lanthanum nickelate is close to that of praseodymium compound. Inspection of the phase diagram[58] shows that the $Pr_2NiO_{4+\delta}$ compound with $\delta=0.22$ lies outside the composition range where stripes are observed, whereas the compound with $\delta=0.11$ studied here lies inside. It is therefore tempting to assign the very unusual shoulders observed here in the low-frequency tails of phonon bands not only to polaronic effects, as previously suggested in Refs. 47, 49, and 57, but more specifically to a peculiar arrangement of charges bounded to the lattice in the form of a multipolaronic stripe. In addition, since this additional spectral weight does not contribute to the zero-frequency conductivity (which is negligible), we may suggest the signature of static charge stripes. On the other hand, the midinfrared bump that is observed in many oxide conductors, inside and outside the stripe phases, is assigned to isolated trapped polarons.

Figure 10 displays the temperature dependence of the phonon dampings. Again a change of regime is observed near 90 K. Damping reflects complicated interactions, including phonon-phonon and phonon-electron interactions. Taking into account the combined spin and charge orders that occurs below 90 K, the question of the possible further interactions of phonons with spins is raised. The strong coupling between transport and magnetic properties was already addressed in Ref. 21.

We come back to the very unusual asymmetric shape of peaks at 4 K. In our opinion, the most original results of this work is displayed in Fig. 11. To find the origin of the shoulders, we have attempted to fold the phonon dispersion curves obtained on a $La_2NiO_4$ single crystal by two of the present authors.[59] *All the additional small peaks forming the shoulders almost exactly fit the folding at wave vector* $Q=0.285\pm0.015$ *propagating in the (110) direction*, as seen in Fig. 12. Such a $Q$ value is incommensurate with the lattice. The magnitude of peaks resulting from such a folding infers the stripes. Shoulders were suggested (in particular by the Fano antiresonance) but hardly seen in the report of Ref. 37. The $Q$ value found here is consistent with the electronic concentration deduced from oxygen overstoichiometry.[16] The feature at 575 cm$^{-1}$ in Fig. 11 appears as a hole instead of a peak. This is the same mode that gave rise to large Fano antiresonance in Ref. 37: it infers the conducting character of the stripes and, therefore, the irrelevance of the low-frequency charge gap.

## CONCLUSION

We have studied the anomalous behavior of lanthanum nickelate for a hole concentration belonging to a phase in which other characterizations suggest the existence of stripes. We confirm two anomalies which are attributed to a change of regime from mobile to trapped polarons upon cooling, and to isolated polarons to multipolarons (static stripes), confirming the combined charge and spin order reported at low temperature by other methods. We have analyzed the many additional small peaks observed in the optical conductivity measured at 4 K in terms of folding of the incommensurate $Q=(0.285,0.285,0)$ wave vector at the zone center. More systematic studies of the optical conductivity versus oxygen excess in nickelates are highly desirable to exploit the amazing phenomenon reported and analyzed here, that appears as an almost direct additional way to characterize stripes.

*Email address: reveau@univ-tours.fr.

[1] J. M. Tranquada, B. J. Sternlieb, J. D. Axe, Y. Nakamura, and S. Uchida, Nature (London) **375**, 561 (1995).

[2] C. H. Chen, S.-W. Cheong, and A. S. Cooper, Phys. Rev. Lett. **71**, 2461 (1993).

[3] Y. Moritomo, Y. Tomioka, A. Asamitsu, Y. Tokura, and Y. Matsui, Phys. Rev. B **51**, 3297 (1995).

[4] Z. Hiroi, T. Obata, M. Takano, and Y. Bando, Phys. Rev. B **41**, 11 665 (1990).

[5] J. M. Tranquada, Y. Kong, and J. E. Lorenzo, Phys. Rev. B **50**,

6340 (1994).
[6] J. M. Tranquada, J. E. Lorenzo, D. J. Buttrey, and V. Sachan, Phys. Rev. B **52**, 3581 (1995).
[7] T. Kyômen, M. Oguni, M. Itoh, and K. Kitayama, Phys. Rev. B **60**, 815 (1999).
[8] V. J. Emery and S. A. Kivelson, Physica C **235–240**, 189 (1994).
[9] J. M. Tranquada, D. J. Buttrey, and V. Sachan, Phys. Rev. B **54**, 12 318 (1996).
[10] S. Q. Shen and Z. D. Wang, Phys. Rev. B **58**, 8877 (1998).
[11] J. M. Tranquada, J. D. Axe, N. Ichikawa, A. R. Moodenbaugh, Y. Nakamura, and S. Uchida, Phys. Rev. Lett. **78**, 338 (1997).
[12] J. M. Tranquada, J. D. Axe, N. Ichikawa, Y. Nakamura, S. Uchida, and B. Nachumi, Phys. Rev. B **54**, 7489 (1996).
[13] P. G. Radaelli, J. D. Jorgensen, R. Kleb, B. A. Hunter, F. C. Chou, and D. C. Johnston, Phys. Rev. B **49**, 6239 (1994).
[14] T. Katsufuji, T. Tanabe, T. Ishikawa, Y. Fukuda, T. Arima, and Y. Tokura, Phys. Rev. B **54**, 14 230 (1996).
[15] V. Sachan, D. J. Buttrey, J. M. Tranquada, J. E. Lorenzo, and G. Shirane, Phys. Rev. B **51**, 12 742 (1995).
[16] H. Yoshizawa, T. Kakeshita, R. Kajimoto, T. Tanabe, T. Katsufuji, and Y. Tokura, Phys. Rev. B **61**, 854 (2000).
[17] S. M. Hayden, G. H. Lander, J. Zarestsky, P. J. Brown, C. Stassis, P. Metcalf, and J. M. Honig, Phys. Rev. Lett. **68**, 1061 (1992).
[18] J. M. Tranquada, D. J. Buttrey, V. Sachan, and J. E. Lorenzo, Phys. Rev. Lett. **73**, 1003 (1994).
[19] S.-W. Cheong, C. H. Chen, H. Y. Hwang, B. Batlogg, L. W. Rupp, Jr., and A. S. Cooper, Physica B **199–200**, 659 (1994).
[20] P. Odier, N. J. Poirot, P. Simon, and D. Desousa Meneses, Eur. Phys. J. A **5**, 123 (1999).
[21] N. J. Poirot, P. Odier, and P. Simon, J. Alloys Compd. **262–263**, 147 (1997).
[22] J. G. Berdnorz and K. A. Müller, Z. Phys. B: Condens. Matter **64**, 189 (1986).
[23] C. Chaillout, S. I. V. Cheong, Z. Fisk, M. S. Lehman, M. Marezo, B. Morosin, and J. E. Schirber, Physica C **158**, 183 (1989).
[24] J. D. Jorgensen, B. Dabrowski, S. Pei, D. R. Richards, and D. G. Hinks, Phys. Rev. B **40**, 2187 (1989).
[25] Y. Takeda, R. Kanno, M. Sakano, O. Yamamoto, M. Takano, Y. Bando, H. Akinaga, K. Takita, and J. B. Goodenough, Mater. Res. Bull. **25**, 293 (1990).
[26] K. Sreedhar and J. M. Honig, J. Solid State Chem. **111**, 147 (1994).
[27] T. Kyômen, M. Oguni, M. Itoh, and K. Kitayama, Phys. Rev. B **60**, 14 841 (1999).
[28] B. J. Sternlieb, J. P. Hill, U. C. Wildgruber, G. M. Luke, B. Nachumi, Y. Moritomo, and Y. Tokura, Phys. Rev. Lett. **76**, 2169 (1996).
[29] Y. Murakami, H. Kawada, M. Tanaka, T. Arima, Y. Moritomo, and Y. Tokura, Phys. Rev. Lett. **80**, 1932 (1998).
[30] J. M. Tranquada, Ferroelectrics **177**, 43 (1996).
[31] P. Wochner, J. M. Tranquada, D. J. Buttrey, and V. Sachan, Phys. Rev. B **57**, 1066 (1998).
[32] Y. S. Yi, Z. G. Yu, A. R. Bishop, and J. T. Gammel, Phys. Rev. B **58**, 503 (1998).
[33] R. J. McQueeney, A. R. Bishop, Ya-Sha, and Z. G. Yu, J. Phys.: Condens. Matter **12**, L317 (2000).
[34] J. M. Tranquada, P. Wochner, A. R. Moodenbaugh, and D. J. Buttrey, Phys. Rev. B **55**, 6113 (1997).
[35] G. Blumberg, M. V. Klein, and S.-W. Cheong, Phys. Rev. Lett. **80**, 564 (1998).
[36] K. Yamamoto, T. Katsufuji, T. Tanabe, and Y. Tokura, Phys. Rev. Lett. **80**, 1493 (1998).
[37] Yu. G. Pashkevivh, V. A. Blinkin, V. P. Gnezdilov, V. V. Tsapenko, V. V. Eremenko, P. Lemmens, M. Fischer, M. Grove, G. Güntherodt, L. Degiorgi, P. Wachter, J. M. Tranquada, and D. J. Buttrey, Phys. Rev. Lett. **84**, 3919 (2000).
[38] J. Zaanen and P. B. Littlewood, Phys. Rev. B **50**, 7222 (1994).
[39] P. Calvani, M. Capizzi, S. Lupi, P. Maselli, A. Paolone, and P. Roy, Phys. Rev. B **53**, 2756 (1996).
[40] R. P. S. M. Lobo, F. J. Gotor, P. Odier, and F. Gervais, Phys. Rev. B **53**, 410 (1996).
[41] Y. Yagil and E. K. H. Salje, Physica C **256**, 205 (1996).
[42] J. P. Falk, A. Levy, M. A. Kastner, and R. J. Birgeneau, Phys. Rev. B **48**, 4043 (1993).
[43] X. X. Bi, P. C. Eklund, and J. M. Honig, Phys. Rev. B **48**, 3470 (1993).
[44] D. M. Eagles, R. P. S. M. Lobo, and F. Gervais, Phys. Rev. B **52**, 6440 (1995).
[45] K. Dembinski, J. M. Bassat, J. P. Coutures, and P. Odier, J. Mater. Sci. Lett. **6**, 1365 (1987).
[46] F. Gervais, P. Echegut, J. M. Bassat, and P. Odier, Phys. Rev. B **37**, 9364 (1988).
[47] S. Lupi, P. Maselli, M. Capizzi, P. Calvani, P. Giura, and P. Roy, Phys. Rev. Lett. **83**, 4852 (1999).
[48] R. P. S. M. Lobo, F. Gervais, C. Champeaux, P. Marchet, and A. Catherinot, Mater. Sci. Eng., B **34**, 74 (1995).
[49] R. P. S. M. Lobo, F. Gervais, and S. B. Oseroff, Europhys. Lett. **37**, 341 (1997).
[50] J. F. Baumard and F. Gervais, Phys. Rev. B **15**, 2316 (1977).
[51] N. Petit, J. C. Soret, and F. Gervais, Solid State Commun. **110**, 621 (1999).
[52] N. Petit, C. Daulan, J. C. Soret, A. Maignan, and F. Gervais, Eur. Phys. J. B **14**, 617 (2000).
[53] F. Gervais, in *Infrared and Millimeter Waves*, edited by K. J. Button (Academic Press, New York, 1983), Vol. 8, Chap. 7, Tableau 1.
[54] D. N. Basov, C. C. Homes, E. J. Singley, M. Strongin, T. Timusk, G. Blumberg, and D. Van der Marel, Phys. Rev. B **63**, 134514 (2001).
[55] T. Startseva, T. Timusk, A. V. Puchkov, D. N. Basov, H. A. Mook, M. Okuya, T. Kimura, and K. Kishio, Phys. Rev. B **59**, 7184 (1999).
[56] J. J. McGuire, M. Windt, T. Startseva, T. Timusk, D. Colson, and V. Viallet-Guillen, Phys. Rev. B **62**, 8711 (2000).
[57] S. Lupi, P. Calvani, M. Capizzi, and P. Roy, Phys. Rev. B **62**, 12418 (2000).
[58] Ch. Allançon, P. Odier, J. M. Bassat, and J. P. Loup, J. Solid State Chem. **131**, 167 (1997).
[59] L. Pintschovius, J. M. Bassat, P. Odier, F. Gervais, G. Chevrier, W. Reichardt, and F. Gompf, Phys. Rev. B **40**, 2229 (1989).